Article

JOURNAL OF COMPOSITE MATERIALS

Journal of Composite Materials
2016, Vol. 50(25) 3539–3550

DOI: 10.1177/0021998315622247
jcm.sagepub.com

SAGE

Pull-out behavior of natural fiber from earth-based matrix

Kabiru Mustapha[1,2], Salifu T Azeko[1,3], Ebenezer Annan[1,4], Martiale G Zebaze Kana[2], Leo Daniel[5] and Winston O Soboyejo[1,6,7]

Abstract

This paper presents the results of a combined experimental and analytical study of the pull-out behavior of natural fiber (grass straw) from an earth-based matrix. A single fiber pull-out approach was used to measure interfacial properties that are significant to toughening brittle materials via fiber reinforcement. This was used to study the interfacial shear strengths of straw fiber-reinforced earth-based composites with a matrix that consists of 60 vol. % laterite, 20 vol. % clay and 20 vol. % cement. The composites that were used in the pull-out tests included composites reinforced with 0, 5, 10 and 20 vol. % of straw fibers. The toughening behavior of fiber-reinforced earth-based matrix was analyzed in terms of their interfacial shear strengths and bridging zones, immediately behind the crack tip. This approach is consistent with microscopic observations that reveal intact bridging fibers behind the crack tip, as a result of debonding of the fiber–matrix interface. Analytical models were used to study the debonding of fiber from the matrix materials, as well as the toughening due to crack-tip shielding via bridging. The results show that increasing the fiber embedment length and the fiber volume fraction (in the earth/cement matrix) increases the peak pull-out load. The debonding process was also found to be associated with a constant friction stress. The combined effects of multiple toughening mechanisms (debonding and crack bridging) are elucidated along with the implications of the results for the design of earth-based composites for potential applications in robust building materials for sustainable eco-friendly homes.

Keywords

Fiber pull-out, interface, debonding, friction stress, crack bridging, toughening mechanisms

Introduction

Recent studies in the area of infrastructural materials have focused largely on development of fiber reinforced composites that provide improved fracture toughness, compared to their matrix materials.[1] The toughening provided by fibers (in fiber-reinforced composites) via crack bridging and other mechanisms, depends significantly on the properties of the matrix, fibers, and the interface(s) between the matrix and fibers.[2] The interfacial shear strength between the matrix and the fibers is often the key to composite toughening and fracture properties.[3] Prior work has also shown that the best overall toughening of ceramic matrix composite may require debonding and frictional sliding to occur at the interfaces between the fibers and matrix.[4–7]

Several studies have been carried out to examine the effects of bonding properties between fibers and matrix on the overall toughness of composite materials. These

[1]Department of Materials Science and Engineering, African University of Science and Technology, Abuja, Nigeria
[2]Department of Materials Science and Engineering, College of Engineering and Technology, Kwara State University, Malete, Nigeria
[3]Department of Civil Engineering, Nigerian Turkish Nile University, Abuja, Nigeria
[4]Department of Materials Science and Engineering, University of Ghana, Accra, Ghana
[5]Department of Aeronautic and Astronautic Engineering, College of Engineering and Technology, Kwara State University, Malete, Nigeria
[6]Department of Mechanical and Aerospace Engineering, Princeton University, Olden Street, Princeton, NJ, USA
[7]Princeton Institute of Science and Technology of Materials (PRISM), Princeton University, Princeton, NJ, USA

Corresponding author:
Winston O Soboyejo, Department of Mechanical and Aerospace Engineering, Princeton University, Olden Street, Princeton, NJ 08544, USA.
Email: soboyejo@princeton.edu

studies focus on interfacial tensile strength,[8,9] interfacial shear strength[10–12] or the combined stress state of normal and shear.[13,14] An investigation by Kim et al.[2] involving pull-out behavior in concrete reinforced with steel, PP and PVA fibers showed that the structure of fibers in the interface changed the bond behavior and bond strengths. Similar observations were also reported by Mazaheripour et al.[15] and Won et al.[16] These studies have shown that the initial elastic deformation is truncated by load drops, corresponding to the onset of interfacial debonding. This is followed by fiber pull-out, during which frictional stresses and residual clamping stresses resist the pull-out of the fibers from the matrix materials.

In brittle-matrix composites, the interfacial shear strengths are often characterized by the debond stress or the frictional pull-out stress.[17] The interfacial shear strengths also have strong effects on composite strength and composite fracture toughness.[18] This has motivated several researchers to study the fiber/matrix interface properties in such composites. An investigation by Mendell et al.[19] focused on the determination of the force required to slip a fiber through a matrix. Other researchers[20,21] used fiber pull-out tests to measure the interfacial shear strengths. The effects of fiber surface conditions (on bond strength) have been studied by Rose and Russel.[22] They reported that a roughened fiber surface improves the interfacial bond strength. Another investigation by Chao et al.[23] explored the bond behavior of un-tensioned strands embedded in concrete reinforced with various fiber volume fractions. Their results showed that pull-out behavior of strands was improved for a concrete matrix with 1% fiber volume fraction.

In modeling the fiber pull-out, the characterization of the frictional stress (at the interface of the fiber-matrix mix) has been an open issue for a long time.[24] Most studies have focused directly on measuring frictional stresses using theoretical models that are guided by experimental observations and measurements. Hence, depending on experimental results, most authors assume either a constant frictional stress or Coulomb friction.[25]

Fiber pull-out has also been studied extensively in advanced composites for potential applications in the aerospace, automotive and energy industries.[26–28] However, there have been no prior studies of the interfacial shear strengths of natural fiber-reinforced earth-based composites that are being developed for structural applications in affordable housing. Hence, the present study will explore the interfacial shear strengths of natural fiber-reinforced earth-based (straw fiber) composites using the single-fiber pull-out test. The fiber pull-out tests will be used to determine the effects of fiber embedment length and fiber volume fraction. The toughening resulting from fiber pull-out and crack bridging will also be elucidated using a combination of experiments and theoretical models.

Materials

Natural fiber-reinforced earth-based composites were produced from locally sourced materials obtained directly from their deposition sites in Abeokuta, Ogun State, South-West Nigeria. These included: laterite (lateritis),[29] clay (which was used as a stabilizer) and straw fibers obtained from dried grass (*Andropogon virginicus*).[30] The fine-grained, clay (consisting primarily of hydrated silicates of aluminum with traces of iron oxide) also serves as a binder in the predominantly lateritic matrix.[31] Type I Ordinary Portland cement was procured from Lafarge Cement Factory, Ewekoro, Ogun State, Nigeria. The cement was also used as a binder.

Sample preparation

The specimens used had rectangular shapes with dimension of 12.5 mm × 25 mm × 100 mm for the single edge notched bend (SENB) test and 25 mm × 25 mm × 100 mm for the fiber pull-out tests. Grass straws with diameters ranging from of 1.90 to 2.10 mm were cut into whiskers with lengths of 10 mm. These were used as reinforcements (randomly oriented) in the predominantly earth-based matrix.

Matrix materials and the grass straws were dry-mixed manually with the aid of a hand trowel. This was done for about 2 min (for homogenization), followed by the addition of water at a water–cement ratio of 1:2. The mixtures were then molded into the stipulated shapes. For fiber pull-out specimens, the surfaces of the fibers were cleaned and the fibers were embedded at the center of the specimen. The natural fibers were then aligned with a fixture, without any significant pre-tension, prior to molding. Three different fiber embedment lengths: 15 mm, 20 mm and 25 mm were considered, along with four different fiber volume fractions (0%, 5%, 10% and 20%) in the matrix.

The samples were then prepared in a mold using a hydraulic press that was operated at a pressure of 2 MPa for 5 min. Pressure values between 1 MPa and 3 MPa were tried initially before settling for a pressure value of 2 MPa, which produced the best compacted samples. SENB specimens were used for the ASTM E399 standard fracture toughness tests. These were produced by machining notches (with notch length to width ratios of 0.40–0.45) into the samples. After molding, the specimens were air dried at room temperature ($\sim$ 25°C) with average relative humidity of 80% for

28 days. For each matrix and composite formulation, 10 specimens were prepared.

Experimental procedures

Chemical and physical characterization of the raw materials used was carried out, respectively, using energy dispersive X-ray spectroscopy (EDS) analysis and particle size distribution measurements. An Instron 3360 series (Norwood, MA, USA) electro-mechanical universal tensile testing machine was used to carry out single fiber pull-out and SENB fracture toughness tests. The underlying crack/microstructure interactions were observed using an in situ optical microscope (Model AY11336, Barska, Pomona, CA, USA). The fracture surfaces of natural fiber-reinforced earth-based composites were also characterized using a Carl Zeiss MA-10 scanning electron microscope (SEM).

The stage for the fiber pull-out experiment is presented schematically in Figure 1(a). This was used for the measurement of the interfacial shear strengths of natural fiber-reinforced earth-based composites. The effects of fiber embedment length and fiber volume fraction (on the fiber pull-out characteristics) were considered. Ten replicates were tested for each embedment length at different fiber volume fractions. Plots of load versus displacement were obtained for various embedment lengths at a loading rate of 3.3 N/s. The samples were tested at room temperature with average a relative humidity of 65%. The other ends of the embedded fibers were held firmly by tension wedge grips attached to a 2 kN load cell, while the specimen was fixed securely to the Instron electro-mechanical testing machine with the aid of G-clamps, as shown in Figure 1(b). The fiber displacement was monitored with an *in situ* optical microscope.

The fracture toughness, K_c, of earth-based matrix and composite were measured using SENB fracture mechanics specimens. This was obtained from[32]

$$K_c = F(a/w)\sigma_f\sqrt{\pi a} \tag{1}$$

where $F(a/w)$ is a compliance function, σ_f is the flexural stress at the peak load and 'a' is the crack length. The compliance function for the SENB specimen can be obtained in the ASTM E399–90[33]

$$F\left(\frac{a}{w}\right) = \frac{3\left(\frac{a}{w}\right)^{\frac{1}{2}}}{2\left(1+2\frac{a}{w}\right)\left(1-\frac{a}{w}\right)^{\frac{3}{2}}} \times \left[\begin{array}{l} 1.99 - \left(\frac{a}{w}\right)\left(1-\frac{a}{w}\right) \\ \left(2.15 - 3.93\frac{a}{w} + 2.7\frac{a^2}{w^2}\right) \end{array}\right] \tag{2}$$

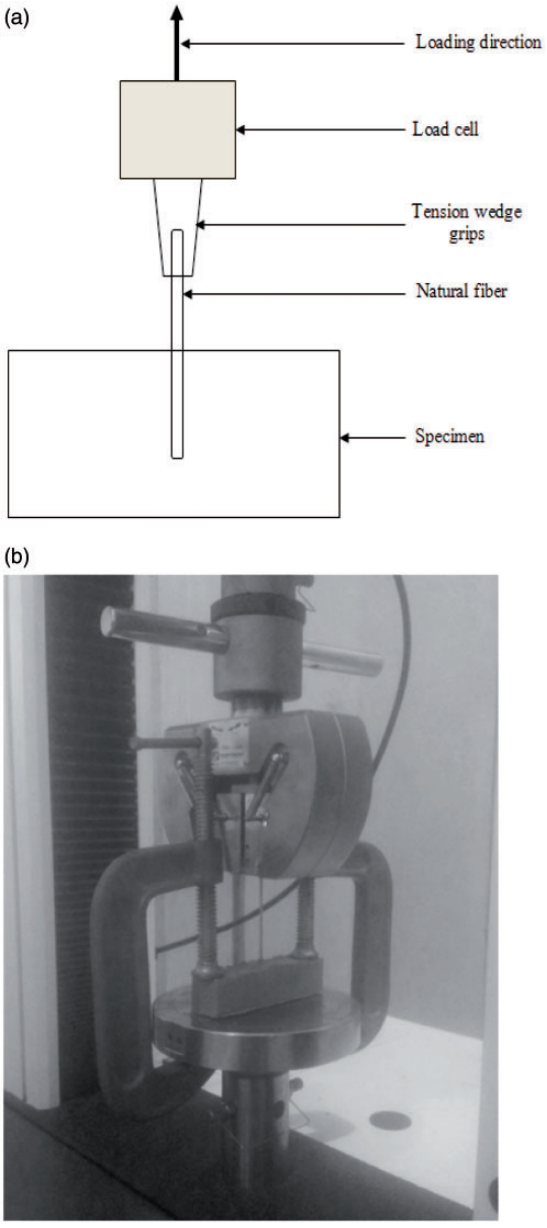

Figure 1. (a) Schematic diagram of the fiber pull-out set-up and (b) experimental setup for Pull-out of natural fiber from earth-based cementitious matrix.

Modeling

Modeling of fiber pull-out (debonding with constant friction)

A model proposed originally by Hutchinson and Jensen[25] was used in this study. This model, which assumes a constant friction stress between fiber and matrix, was adopted to model the effects of fiber pull-out on the toughening of earth-based composites. In this model, the composite system consists of a fiber (radius r_f) within a cylindrical outer boundary of

radius r (Figure 2). The area fraction of the fiber is taken as $\rho = (r_f/r)^2$ and the average stress in the fiber varies according to

$$d\sigma_f/dz = (2/r_f)\tau \quad (3)$$

where σ_f is the average axial stress in the fiber, r_f is the radius of the fiber and τ is friction stress between the matrix and the fiber. Equation (3) is a valid approximation, provided that τ is small compared to σ_f. Also, another essential approximation that was made in the analysis of the model is given by (Figure 5)[25]

For $0 < z < l_o$,

$$\sigma_f = \sigma_f^* + 2\tau(z/r_f) \quad (4)$$

while

$$\sigma_m = \sigma_m^* - 2\rho(1-\rho)^{-1}\tau(z/r_f) \quad (5)$$

where σ_f^* and σ_m^* are the respective fiber and matrix strengths, just below the debond crack tip. If the zero-friction zone shown exists, then
$\sigma_f = \bar{\sigma}/\rho$ and $\sigma_m = 0$ for $l_o < z < l$.

When $\bar{\sigma} < \overline{\sigma_o}$
then $\sigma_f = \bar{\sigma}/\rho$ and $\sigma_m = 0$ at $z = l_o$.

In either case

$$l_o/r_f = \left(\bar{\sigma}/\rho - \sigma_f^*\right)/(2\tau) \quad (6)$$

where $\bar{\sigma}$ is the average axial stress and $\overline{\sigma_o}$ is the maximum value of $\bar{\sigma}$. When a constant frictional stress, τ, exists at the fiber matrix interface and the fiber slides but does not lose contact with the matrix, the variation of toughening, ΔK_2, is approximated by[25]

$$\Delta K_2/\left(\tau r_f^{1/2}\right) = (1-\rho)^{-1/2}(l/r_f) \quad (7)$$

Toughening due to crack bridging

Toughening due to crack bridging (via fiber reinforcement) was also considered using approaches used by Mustapha et al.[34] in earlier work. This was done for small-scale bridging (SSB) and large-scale bridging (LSB). A small-scale bridging model proposed by Budiansky et al.[35] was used for modeling the initial stages of stable crack growth (bridge length < 0.5 mm).

Under SSB conditions, the shielding due to crack bridging ΔK_{SSB} is given by

$$\Delta K_{SSB} = \alpha V_f \sqrt{\frac{2}{\pi}} \int_0^L \frac{\sigma_y}{\sqrt{x}} dx \quad (8)$$

where α is the constraint/triaxiality factor (theoretically between 1 and 3 and taken as ~ 3 in this study),[36] V_f is the volume fraction of the reinforcement phase, L is the bridging length (the distance from the crack-tip to the last unfractured reinforcement), σ_y is the uniaxial yield stress, and x is the distance from the crack face behind the crack-tip as described by Savastano et al.[37]

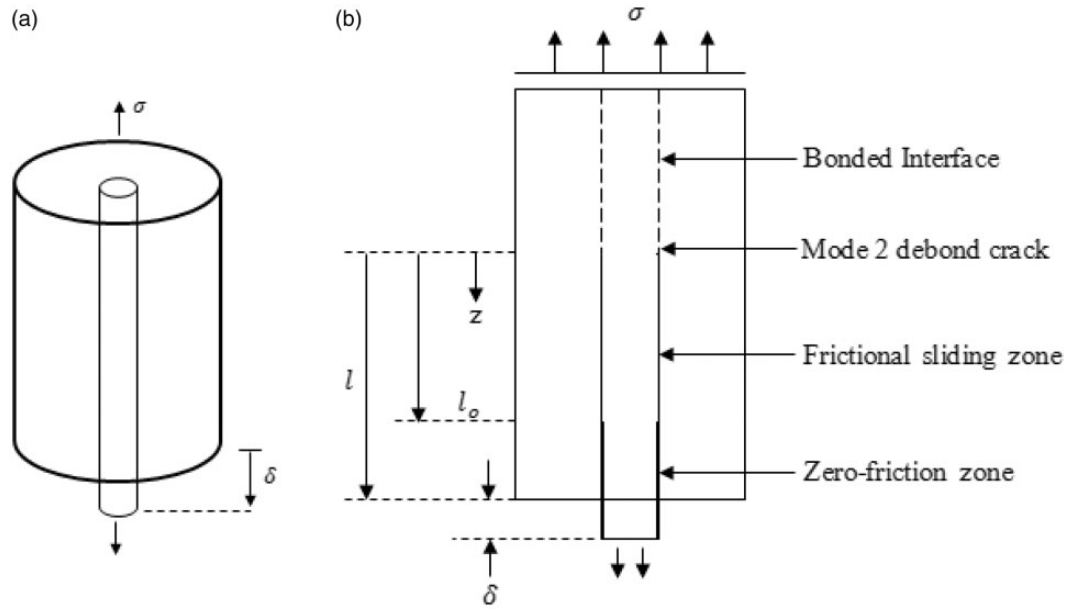

Figure 2. (a) Schematic of fiber debonding and pull-out in a cylindrical cell model and (b) conventions and definitions of fiber debonding and pull-out in a cylindrical cell model.

For large-scale crack bridging (LSB) conditions, the contribution to composite toughness due to crack bridging was also modeled[38,39] using a weighting function by Fett and Munz to estimate the weighted distributions of bridging traction across the crack faces.[40]

Table 1. Summary of Fett and Munz[40] parameters used for single-edged notched bend specimen.

	μ				
ν	0	1	2	3	4
0	0.4980	2.4463	0.0700	1.3187	−3.067
1	0.5416	−5.0806	24.3447	−32.7208	18.1214
2	−0.19277	2.55863	−12.6415	19.7630	−10.986

The shielding from large scale bridging, ΔK_{lsb}, is given by[38]

$$\Delta K_{lsb} = V_f \int_L \alpha \sigma_y h(a, x) \mathrm{d}x \tag{9}$$

where α is the constraint/triaxiality factor (theoretically between 1 and 3 and taken as ~3 in this study),[39] V_f is the volume fraction of the reinforcement phase, L is the bridging length, σ_y is the uniaxial yield stress and x is the distance from the last unfractured fiber to the crack-tip. Also, h(a, x) is the weighting function given by[40]

$$\mathrm{h(a,x)} = \sqrt{\frac{2}{\pi \mathrm{a}}} \frac{1}{\sqrt{1-\frac{\mathrm{x}}{\mathrm{a}}}} \left[1 + \sum_{(\nu,\mu)} \frac{\mathrm{A}_{\nu,\mu}\left(\frac{\mathrm{a}}{\mathrm{W}}\right)}{\left(1-\frac{\mathrm{a}}{\mathrm{W}}\right)} \left(1-\frac{\mathrm{x}}{\mathrm{a}}\right)^{\nu+1} \right] \tag{10}$$

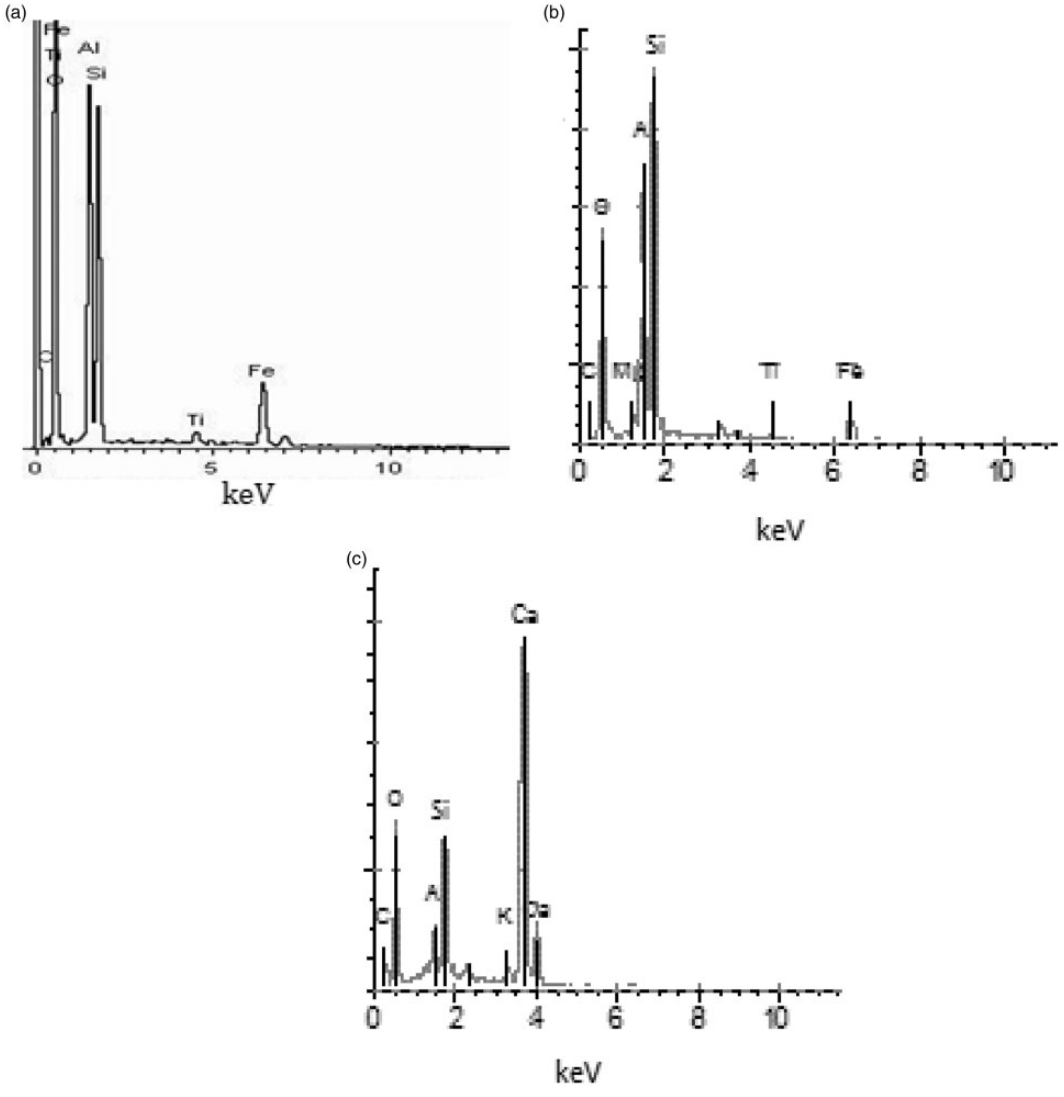

Figure 3. EDS analysis of materials used: (a) laterite (b) clay and (c) ordinary portland cement.

Figure 4. Crack/fiber interaction in stabilized laterite matrix.

where 'a' is the crack length and 'w' is the specimen width. The coefficients $(A_{v,\mu})$ are given in Table 1 for the SENB specimen.

Model for the estimation of shielding due to crack bridging and fiber pull-out

The expression for the estimation of the composite fracture toughness (based on the toughening mechanisms observed in the failure of natural fiber-reinforced earth-based composite) is given by[34]

$$K_R = K_i + \Delta K \tag{11}$$

where K_R is the composite fracture toughness and ΔK is the shielding due to crack bridging and fiber pull-out. For toughening due to fiber pull-out at constant frictional stress, $\Delta K = \Delta K_2$ and for bridging toughening, $\Delta K = \Delta K_1$ (for a combined small- and large- scale bridging).

In this study, multiple toughening mechanisms were observed. Hence, the overall toughening was estimated from the contributions due to both mechanisms. A linear superposition model, which neglected the possible interactions between the individual toughening mechanisms, was used. However, synergistic relationships between the toughening mechanisms provide more realistic estimates of composite toughening than the individual toughening components.[41] For toughening by crack bridging and fiber pull-out with constant fractional stress, the overall toughening is given by[42]

$$\Delta K = \lambda \Delta K_1 + (1 - \lambda)\Delta K_2 \tag{12}$$

where ΔK is the total toughening, λ is the toughening ratio due to crack bridging, ΔK_1 and ΔK_2 are the toughening due to crack bridging and fiber pull-out, respectively.

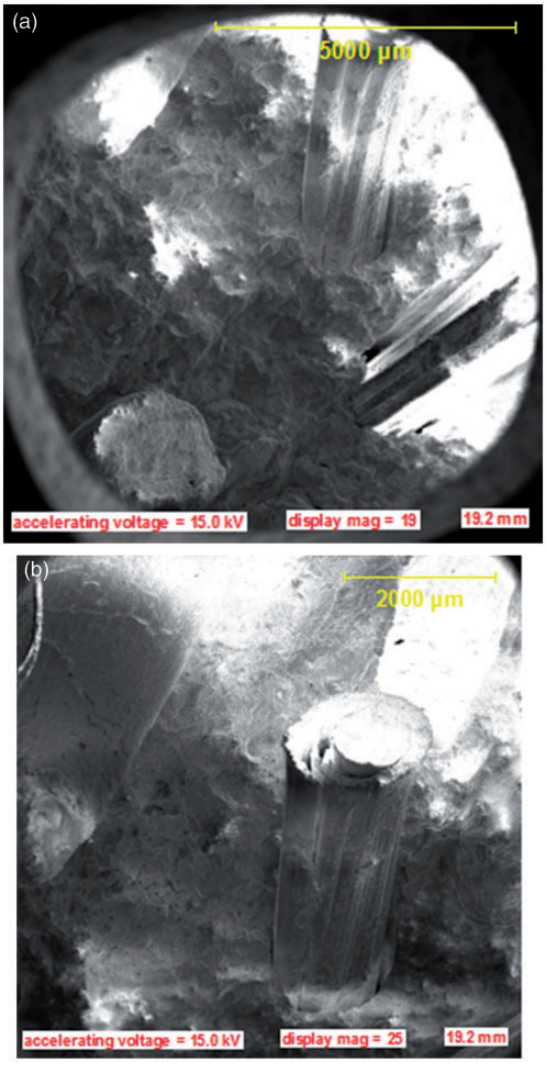

Figure 5. SEM images of fracture surfaces showing evidence of debonding and fiber pull-out.

Results and discussion

Material characterization

Laterite, clay and Ordinary Portland Cement (OPC) with respective maximum particle sizes of 250 microns, 150 microns and 74 microns, were used in this study. These particle sizes were obtained by measuring and converting mesh sizes of the sieves into microns. Figure 3 shows the energy dispersive X-ray spectroscopy analysis of the materials that were used. The elemental compositions obtained are consistent with prior studies.[43–46] The interactions of the cracks with straw fibers are shown in Figure 4. This shows clear evidence of crack bridging, while the scanning microscopy

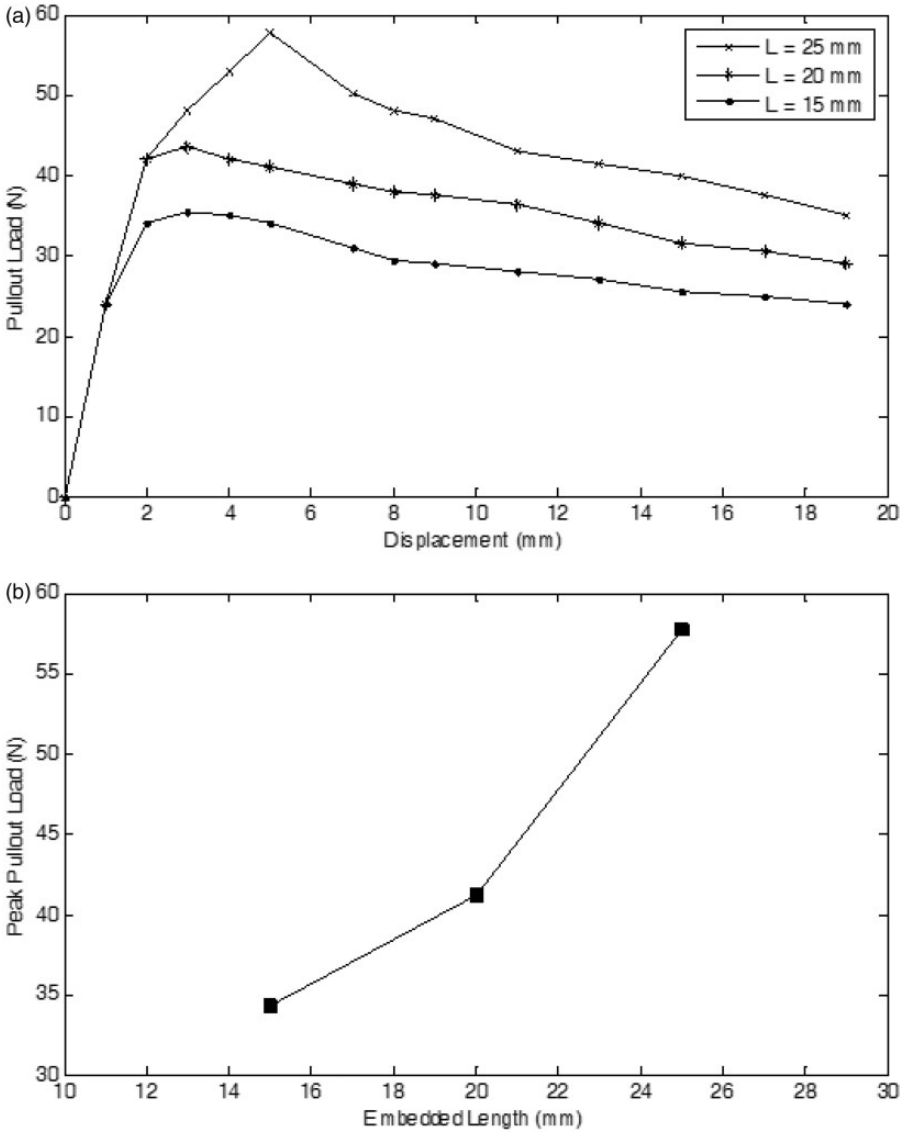

Figure 6. (a) Effect of embedment length on the pull-out behavior of natural fiber from earth-based cementitious matrices and (b) effect of fiber embedment length on peak pull-out load.

images (Figure 5) reveal evidence of intact fiber pull-out on fracture surfaces.

Single fiber pull-out

The results of the single fiber pull-out experiments are presented in Figures 6–8. The pull-out curves obtained in this study can be divided into three regimes, as presented in prior work on other ceramic matrix composites.[47,48] These include (i) a linear elastic deformation stage; (ii) a partial fiber debonding stage, and (iii) a frictional pull-out stage. Frictional bond strengths were also calculated by dividing the maximum pull-out load by the embedded fiber surface area. The resulting interfacial shear strengths were used to predict the maximum contributions of the fiber pull-out loads to the composite fracture toughness values.

Figure 6(a) shows the effects of embedment length on the peak pull-out loads. A significant increase was observed in the peak pull-out load (while keeping other parameters constant) with increasing fiber embedment length (from 15 mm to 25 mm). This is attributed to the increase in the fiber/matrix contact area that occurs with increasing fiber embedment length. Similar observations have also been reported by Wang et al.[4] and Baran et al.[5]

Meanwhile, Figure 6(b) shows that the peak pull-out load does not appear to be directly proportional to the fiber embedment length. This is because the onset of fiber debonding corresponds to the condition at which

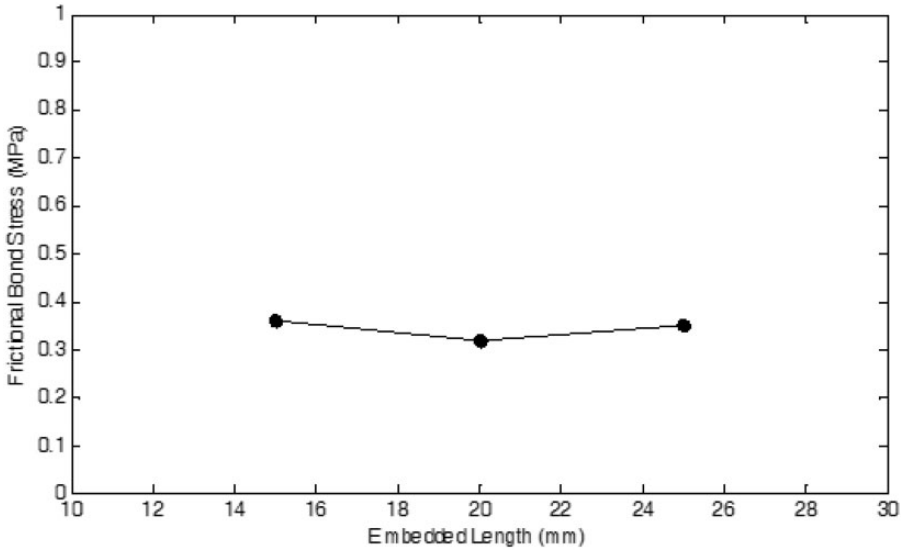

Figure 7. Effect of fiber embedment length on frictional bond strength for earth-based cementitious matrices.

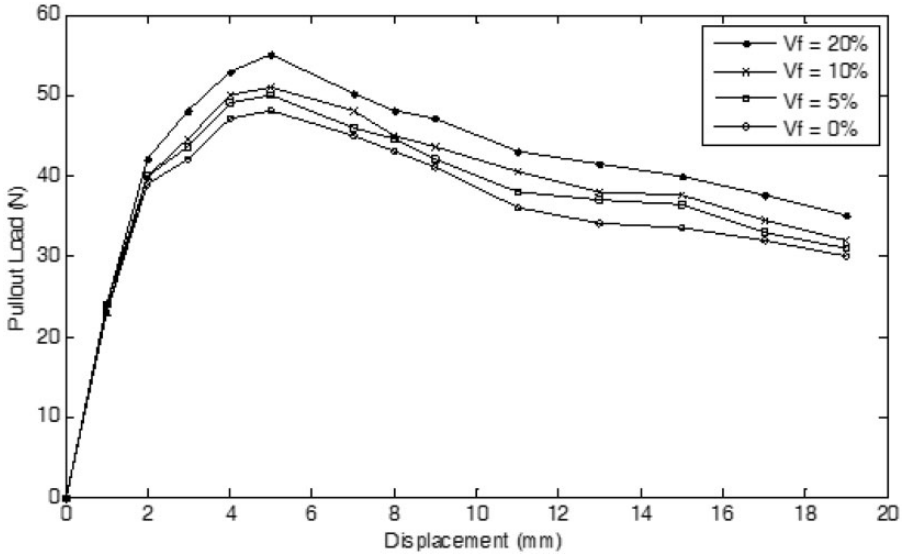

Figure 8. Effect of fiber volume fraction on the pull-out of natural fiber from earth-based cementitious matrices.

the interfacial crack driving force is equal to the interfacial fracture toughness at the local mode mixity. Since this depends non-linearly on the internal crack lengths and elastic properties of the materials, the fiber pull-out loads are unlikely to exhibit a linear dependence of the fiber embedment length.

The results (Figure 7) showed that fiber pull-out occurred with a constant frictional bond stress at the interface between the fiber and earth-based cementitious matrices. This formed the basis for the model considered to predict composite toughening due to fiber pull-out. An average frictional bond strength of about 0.34 ± 0.02 MPa was obtained for earth-based cementitious matrix. Other results obtained for composites (with varying fiber volume fractions) will be used in the next section to predict the toughening due to the same mechanism.

Figure 8 shows the fiber pull-out strengths obtained for fiber volume percentages between 0 and 20. The fiber pull-out loads increased with increasing fiber volume fraction. This increase in the pull-out load was attributed to the increase in the fiber bundle/composite ligament strengths that occurs with increasing fiber volume fraction. This also results in fiber interlocking, which provides additional resistance to fiber pull-out. It also resulted in a reduction of frictional decay, as obtained by Chao et al.[23] Hence, the increase in the volume fraction of fibers provides

Table 2. Fracture toughness results obtained from experiments.

Volume percentages of reinforcement	$K_c(MPa\sqrt{m})$
0 vol% Fiber	1.07 ± 0.05
5 vol% Fiber	1.23 ± 0.06
10 vol% Fiber	1.28 ± 0.07
20 vol% Fiber	1.41 ± 0.11

Table 3. Predicted toughening due to fiber pull-out (ΔK_2) model.

Volume percentages of reinforcement	τ (MPa)	r_f (m)	r (m)	P	ΔK_2 $(MPa\sqrt{m})$
5 vol% Fiber	0.39 ± 0.02	0.001	0.002	0.25	0.13 ± 0.01
10 vol% Fiber	0.40 ± 0.02	0.001	0.002	0.25	0.17 ± 0.01
20 vol% Fiber	0.44 ± 0.02	0.001	0.002	0.25	0.29 ± 0.01

τ = Friction stress between the matrix and the fiber; r_f = radius of the fiber; r = radius of cylindrical outer boundary of matrix; ρ = area fraction of the fiber.

Table 4. Predicted toughening due to crack bridging (ΔK_1) model.

Volume percentages of reinforcement	V_b	L (mm)	α	ΔK_1 $(MPa\sqrt{m})$
5 vol% Fiber	0.050	4.5	3	0.21 ± 0.01
10 vol% Fiber	0.075	4.5	3	0.29 ± 0.01
20 vol% Fiber	0.100	4.5	3	0.43 ± 0.02

V_b = Fiber volume fraction in the bridge zone; L = length of the bridge zone; α = triaxiality factor.

increased the shielding due to crack bridging and fiber pull-out.

Composite toughening

The results of the fracture toughness tests obtained experimentally from SENB tests are presented in Table 2. An initiation toughness of 1.07 ± 0.05 $MPa\sqrt{m}$ was obtained for the composition considered in this study. The shielding contributions from fiber pull-out and crack bridging models are presented in Tables 3 and 4, respectively, while the results for the combined mechanisms (crack bridging and fiber pull-out) are presented in Table 5. The results show that increasing fiber volume fraction results in increased toughening. Similar observations have also been reported in prior work by Savastano et al. and Agopyan et al., whose studies used vegetable fiber-reinforced cementitious matrices.[49–51] This increase in fracture toughness was attributed primarily to shielding of the crak-tip by the bridging fibers.

Table 5. Predicted toughening due to combined mechanism (fiber pull-out and crack bridging).

Volume percentages of reinforcement	ΔK $(MPa\sqrt{m})$
5 vol% Fiber	0.17 ± 0.01
10 vol% Fiber	0.23 ± 0.01
20 vol% Fiber	0.36 ± 0.02

Note: $\Delta K = \lambda \Delta K_1 + (1 - \lambda)\Delta K_2$; $\lambda = 0.5$

The results also revealed that pull-out (debonding and sliding) and crack bridging interact synergistically in ways that contribute to the overall fracture toughness. The sliding resistance (in this study) is attributed to the rough surface morphology of the fibers.[22] Figure 9 shows that the fracture toughness resulting from the combined mechanisms provided a better estimation of fracture toughness (due to fiber reinforcement), when compared to experimental results obtained in prior work by Mustapha et al.[34]

Implications

The implications of the current study are very significant for the design of composite materials for sustainable and affordable housing. Unlike prior work, which focused primarily on the toughening of earth-based composites due to small/large-scale crack bridging, this paper shows clearly that the overall toughening of earth-based fiber straw composites was due to the combined effects of crack bridging and fiber pull-out. The interactions between these two toughening mechanisms can also be used to engineer improvements of fracture toughness/resistance–curve behavior of earth-based composites.

Further work is clearly needed to optimize the interfaces of coated natural fibers for potential applications in earth-based composites. This suggests that the level of fiber pull-out can be controlled by altering the chemistry of the fibers through coating, or by changing the residual clamping stress.[52,53] Hence, sustainable and low cost housing can be developed using locally available materials with coated fibers that can be used to engineer improvements in the combined effects of crack bridging and fiber pull-out.

Summary and concluding remarks

The interfacial shear strengths and fiber pull-out characteristics have been studied in earth-based composites reinforced with straw fibers. Salient conclusions arising

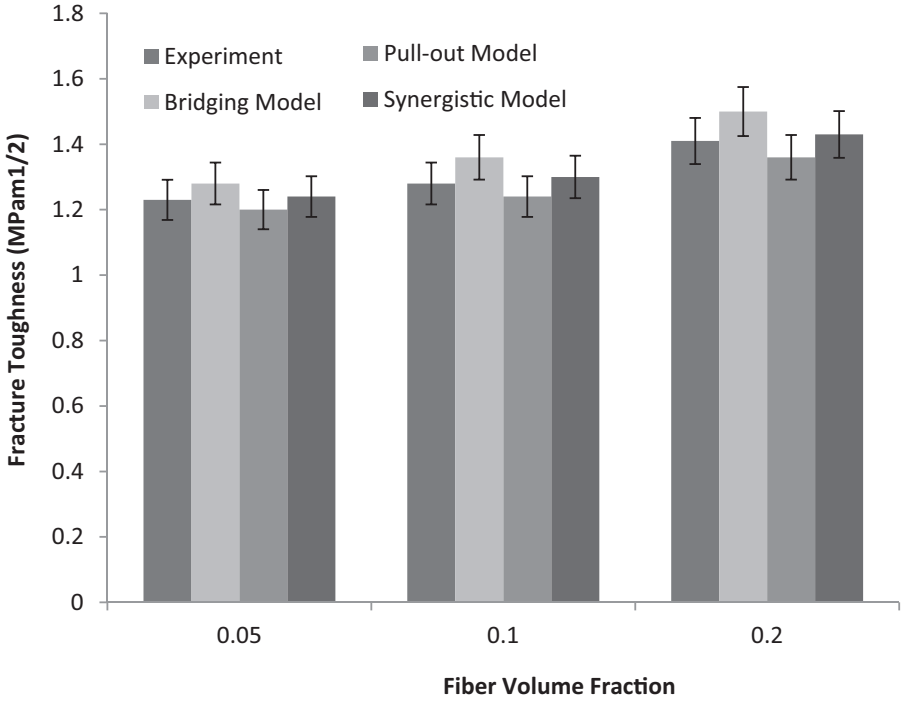

Figure 9. Comparison between experimental results and toughening models.

from the combined experimental and theoretical study are as follows:

i The fiber pull-out strengths increase with increasing fiber embedment length and fiber volume fractions up to 0.2. The measured improvements are consistent with predictions from composite and interfacial fracture models.
ii Following the onset of debonding, a regime of constant frictional pull-out stress is observed. This suggests that the friction stress is not significantly affected by the degree of pull-out.
iii The predicted toughening obtained from the fracture mechanics analyses is consistent with the experimental results. The predictions of fiber bridging and pull-out are consistent with the ranges in the toughening behavior obtained for the earth-based composites with different volume percentages of fibers between 0 and 20 vol. %.
iv The synergistic interactions between individual toughening mechanisms represent a better estimate of toughening than the simple individual toughening components.

Acknowledgments

The authors thank the management and staff of Mateng Nigeria Limited, Abeokuta, and the Materials Science Laboratory, Kwara State University, Malete, for their assistance with the experimental work.

Declaration of Conflicting Interests

The author(s) declared no potential conflicts of interest with respect to the research, authorship, and/or publication of this article.

Funding

The author(s) disclosed receipt of the following financial support for the research, authorship, and/or publication of this article: The authors would like to thank the World Bank African Centers of Excellence Program, the Nelson Mandela Institution and the African University of Science and Technology, Abuja, Nigeria, for funding of this research.

References

1. Savastano H, Santos SF, Radonjic M, et al. Fracture and fatigue of natural fiber-reinforced cementitious composites. *Cem Concr Compos* 2009; 31: 232–243.
2. Kim B, Doh JH, Yi CK, et al. Effects of structural fibers on bonding mechanism changes in interface between GFRP bar and concrete. *Compos Part B* 2013; 45: 768–779.
3. Zhandarov SF and Pisanova EV. Characterization of fiber/matrix interface strength: Applicability of different tests, approaches and parameters. *Compos Sci Technol* 2005; 65: 149–160.
4. Wang H, Sun X, Peng G, et al. Experimental study on bond behaviour between BFRP bar and engineered cementitious composite. *Construct Build Mater* 2015; 95: 448–456.

5. Baran E, Akis T and Yesilmen S. Pull-out behavior of prestressing strands in steel fiber reinforced concrete. *Construct Build Mater* 2012; 28: 362–371.
6. Bouazaoui L and Li A. Analysis of steel/concrete interfacial shear stress by means of pull out test. *Int J Adhes Adhes* 2008; 28: 101–108.
7. Koyanagi J, Nakatani H and Ogihara S. Comparison of glass–epoxy interface strengths examined by cruciform specimen and single-fiber pull-out tests under combined stress state. *Compos Part A: Appl Sci Manuf* 2012; 43: 1819–1827.
8. Koyanagi J, Yoneyama S, Nemoto A, et al. Time and temperature dependence of carbon/epoxy interface strength. *Compos Sci Technol* 2010; 70: 1395–400.
9. Tandon GP and Kim RY. Fiber-matrix interfacial failure characterization using a cruciform-shaped specimen. *J Compos Mater* 2002; 36: 2667–2691.
10. Zhandarov S and Mader E. Characterization of fiber/matrix interface strength: Applicability of different tests, approaches and parameters. *Compos Sci Technol* 2005; 65: 149–160.
11. Yang L and Thomason JL. Interface strength in glass fiber–polypropylene measured using the fiber pull-out and micro bond methods. *Compos Part A* 2010; 41: 1077–1083.
12. Liu Z, Yuan X, Beck AJ, et al. Analysis of a modified micro bond test for the measurement of interfacial shear strength of an aqueous-based adhesive and a polyamide fiber. *Compos Sci Technol* 2011; 71: 1529–1534.
13. Ogihara S and Koyanagi J. Investigation of combined stress-state failure-criterion for glass fiber/epoxy interface by cruciform specimen test. *Compos Sci Technol* 2010; 70: 143–150.
14. Koyanagi J, Shah PD, Kimura S, et al. Mixed-mode interfacial debonding simulation in single fiber composite under a transverse load. *J Solid Mech Mater Eng* 2009; 3: 796–806.
15. Mazaheripour H, Barros JA, Sena-Cruz JM, et al. Experimental study on bond performance of GFRP bars in self-compacting steel fiber reinforced concrete. *Compos Struct* 2013; 95: 202–212.
16. Won JP, Park CG, Kim HH, et al. Effect of fibers on the bonds between FRP reinforcing bars and high-strength concrete. *Compos Part B: Eng* 2008; 39: 747–755.
17. Hsueh CH. Interfacial debonding and fiber pull-out stresses of fiber-reinforced composites. *Mater Sci Eng A* 1990; 123: 1–11.
18. Kim JK and Mai YW. High strength, high fracture toughness fibre composites with interface control—a review. *Compos Sci Technol* 1991; 41: 333–378.
19. Mandell JF, Hong KCC and Grande DH. lnterfacial shear strength and sliding resistance in metal and glass-ceramic matrix composites. In: *Proceeding of the 11th annual conference on composites and advanced ceramic materials*, September 2009, Vol. 8, p.937. John Wiley & Sons.
20. Griffin CW, Limaye SY, Richerson DW, et al. Evaluation of interfacial properties in borosilicate-sic composites using pullout tests. In: *Proceedings of the 12th annual conference on composites and advanced ceramic materials*, Part 1 of 2: 2009, pp.671–678. John Wiley & Sons, Inc.
21. Hsueh CH. Interfacial debonding and fiber pull-out stresses of fiber-reinforced composites III: With residual radial and axial stresses. *Mater Sci Eng A* 1991; 145: 135–142.
22. Rose DR and Russell BW. Investigation of standardized tests to measure the bond performance of prestressing strand. *PCI J* 1997; 42: 56–80.
23. Chao S, Naaman A and Parra-Montesino G. Bond behavior of strand embedded in fiber reinforced cementitious composites. *PCI J* 2006; 51: 56–71.
24. Marshall DB and Evans AG. Failure mechanisms in ceramic-fiber/ceramic-matrix composites. *J Am Ceram Soc* 1985; 68: 225–231.
25. Hutchinson JW and Jensen HM. Models of fiber debonding and pullout in brittle composites with friction. *Mech Mater* 1990; 9: 139–163.
26. Yang Y, Boom R, Irion B, et al. Recycling of composite materials. *Chem Eng Process: Process Intensification* 2012; 51: 53–68.
27. Ashori A. Wood–plastic composites as promising green-composites for automotive industries. *Bio Resource Technol* 2008; 99: 4661–4667.
28. Zhang X, Fan X, Yan C, et al. Interfacial microstructure and properties of carbon fiber composites modified with graphene oxide. *ACS Appl Mater Interface* 2012; 4: 1543–1552.
29. Nandi AK. Laterites-concept, geology, morphology and chemistry. *Geol Soc India* 1995; 46: 451–452.
30. Robert HM. *USDA-NRCS PLANTS Database/USDA SCS. Southern wetland flora: Field office guide to plant species*. Fort Worth: South National Technical Center, 1991.
31. Hillier S. Clay Mineralogy. In: Fairbridge (ed) *Encyclopedia of sediments and sedimentary rocks*. Dordrecht, Netherlands: Kluwer Academic Publishers, 2003, pp.139–142.
32. Callister WD. *Material science and engineering: An introduction*, 7th ed. New York: John Wiley, 2007, pp.414–459.
33. American Society for Testing and Materials. *Standard test method for plane-strain fracture toughness of metallic materials, E399–90*. West Conshohocken: ASTM, 1997, p.31 (Book of Standards v. 03.01).
34. Mustapha K, Annan E, Azeko ST, et al. Strength and fracture toughness of earth-based natural fiber-reinforced composites. *J Compos Mater*. 2016; 50: 1145–1160.
35. Budiansky B, Amazigo JC and Evans AG. Small-scale crack bridging and the fracture toughness of particulate-reinforced ceramics. *J Mesh Phys Solids* 1988; 36: 167–187.
36. Kung E, Mercer C, Allameh S, et al. An investigation of fracture and fatigue in a metal/polymer composite. *Key Eng Mater* 2001; 197: 87–110.
37. Savastano HJ, Turner A, Mercer C, et al. Mechanical behavior of cement-based materials reinforced with sisal fibers. *J Mater Sci* 2006; 41: 6938–6948.

38. Bloyer DR, Ritchie RO and Rao KV. Fracture toughness and R-curve behavior of laminated brittle-matrix composites. *Metal Meter Trans A* 1998; 29: 2483–2496.
39. Bloyer DR, Ritchie RO and Rao KV. Fatigue-crack propagation behavior of ductile/brittle laminated composites. *Metal Meter Trans A* 1999; 30: 633–642.
40. Fett T and Munz D. *Stress intensity factors and weight functions for one-dimensional cracks*. Karlsruhe, Germany: Kernforschungszentrum, 1994.
41. Budiansky B and Amazigo JC. Notch strength of ceramic composites: long fibers, stochastics, short fibers. In: Willis JR (ed.) *Non-linear analysis of fracture*. Dordrecht, The Netherlands: Kluwer, 1997.
42. Shum DKM and Hutchinson W. *On toughening by micro cracks*. Report no. MECH-151 Cambridge, MA: Harvard University, 1989.
43. Kim J, Dodbiba G, Tanno H, et al. Calcination of low-grade laterite for concentration of Ni by magnetic separation. *Mineral Eng* 2010; 23: 282–288.
44. Nyakairu GW and Koeberl C. Mineralogical and chemical composition and distribution of rare earth elements in clay-rich sediments from central Uganda. *Geochem J* 2001; 35: 13–28.
45. Mermut AR and Cano AF. Baseline studies of the clay minerals society source clays: Chemical analyses of major elements. *Clays Clay Mineral* 2001; 49: 381–386.
46. Jo BW, Kim CH, Tae GH, et al. Characteristics of cement mortar with nano-SiO 2 particles. *Construct Build Mater* 2007; 21: 1351–1355.
47. Singh S, Shukla A and Brown R. Pullout behavior of polypropylene fibers from cementitious matrix. *Cem Concr Res* 2004; 34: 1919–1925.
48. Sujivorakul C, Waas AM and Naaman AE. Pullout response of a smooth fiber with an end anchorage. *J Eng Mech* 2000; 126: 986–993.
49. Savastano H Jr and Agopyan V. Transition zone studies of vegetable fibre-cement paste composites. *Cem Concr Compos* 1999; 21: 49–57.
50. Savastano H Jr, Warden PG and Coutts RSP. Brazilian waste fibres as reinforcement for cement-based composites. *Cem Concr Compos* 2000; 22: 379–384.
51. Agopyan V and John VM. Durability evaluation of vegetable fiber reinforced materials: Sisal and coir vegetable fibers as well as those obtained from disintegrated newsprint found to be the most suitable fibers for building purposes. *Build Res Info* 1992; 20: 233–235.
52. Wu J, Yu D, Chan CM, et al. Effect of fiber pretreatment condition on the interfacial strength and mechanical properties of wood fiber/PP composites. *J Appl Polym Sci* 2000; 76: 1000–1010.
53. Monticelli F, Ferrari M and Toledano M. Cement system and surface treatment selection for fiber post luting. *Medicina Oral Patologia Oral y Cirugia Bucal* 2008; 13: 214.